Research article

Corrosion inhibition of mild steel using poly (2-ethyl -2-oxazoline) in 0.1M HCl solution

Zachariah Pulluparampil Mathew [a,b], Keerthi Rajan [a], Cyril Augustine [a], Bincy Joseph [c], Sam John [a,*]

[a] Department of Chemistry, St. Berchmans College (Autonomous) Campus, Mahatma Gandhi University, Kottayam, 686101, India
[b] Department of Chemistry, Rajiv Gandhi Institute of Technology, Kottayam, 686501, India
[c] St. Mary's College, Thrissur, 680020, India

ABSTRACT

Effective inhibition of metallic corrosion to prevent its consequent loss is one of the serious apprehensions for industries in the modern world. This paper analyses the application of poly(2-ethyl-2-oxazoline) (PEOX) as an effective inhibitor of corrosion, when it is made to be in contact with the surfaces of mild steel (MS). The sustainability of MS against corrosion in 0.1 M Hydrochloric acid solution in the presence of known concentration of PEOX is assessed by potentiodynamic polarization (PDP) measurements, linear polarization studies (LPR), and electrochemical impedance spectroscopy (EIS). It was observed that PEOX behaves as better inhibitor for mild steel corrosion in 0.1 M HCl solution and it show enhanced inhibition efficiency (IE%) 79% at a concentration of 50 ppm. The polarization experiments indicated that addition of PEOX in concentrations varies from 25 ppm to 50 ppm induces a decrease of both cathodic and anodic currents densities. Also, the micrographs recorded by the Scanning Electron Microscopy confirm that molecules of PEOX act as corrosion inhibitors for the surfaces of MS in 0.1 M HCl. The stability of the MS surface in a corrosion-prone environment is traced by measuring the contact angles of water droplets placed on the MS surface, to quantify the extent of deterioration, if any, due to corrosion. The results presented here show that the compound PEOX performs as a mixed-type inhibitor against corrosion at the MS surface in acidic medium. Theoretical studies based on the electronic structure of PEOX in aqueous medium also support its performance as a successful corrosion-inhibitor.

1. Introduction

The corrosion from metallic surfaces gives rise to challenges to environmental safety, long-term preservation of materials which are prone to corrosion, waste of energy, gradual degradation of machines and in the safety of the personnel who deal with them. Effective minimization of corrosion becomes an important task as it can compensate to a certain extent the huge economic loss and structural failures in the industries, which are the protuberant consequences of corrosion. The strategies such as cathodic protection, use of protective coatings [1, 2, 3, 4, 5] and corrosion-inhibitors [6, 7, 8] are employed which may alter the mechanism and/or slow down the rate of corrosion from the metallic surfaces.

The corrosion-inhibitors are one of the promising ingredients against corrosion, which are organic or inorganic in nature, and when added in small concentrations can effectively decrease or prevent the reaction of the metallic surfaces with moisture. An ideal inhibitor should be bio-compatible, amenable to treatment and should have the desired action at a high level of accuracy. Hexavalent Chromium and its related compounds, even though found to be one of the most effective inorganic corrosion-inhibitors, are ought to be restricted due to its toxic nature such as carcinogenicity. Conjugated organic molecules with delocalized pi-electrons or those with functionalities containing Nitrogen, Sulphur and Oxygen in conjugation with the π-system have also been reported to exhibit relatively good inhibition against corrosion [9, 10, 11, 12].

Polymer-based organic and inorganic coatings are widely applied [13] for the protection of metallic surfaces prone to corrosive surroundings due to their stability, moderate cost and relatively less toxicity. The performance of the polymeric coatings against the corrosion and the duration of uninterrupted protection are strongly dependent on the composition of the material and its interfacial adhesion to the metallic surface. The pretreatment of metallic surfaces prior to exposing in corrosive environments enhances the adhesion of the polymer at the surface.

A conventional approach to improve the rate of adhesion is to increase the population of the active sites at the metallic surface with abrasive blasting. Consequently, the number of adhesion sites are increased and the traces of extraneous species already adsorbed on the surface are removed. Subsequent formation of a polymer film at the interface between the metal and the electrolyte can effectually inhibit the corrosion by blocking the migration of ions, water and environmental gases to the active anodic and cathodic sites on the metal.

In this research project, poly(2-ethyl-2-oxazoline), PEOX, is used as a substitute for the classical biocompatible polymers such as poly (ethylene glycol), 1-ethenylpyrrolidin-2-one, and poly (hydroxypropyl methacrylate). The PEOX is one of the unique polymers since this is readily soluble in aqueous media and exceptionally biocompatible which makes it suitable for ecofriendly developments. The biocompatibility of the other polymers such as poly(ethylene glycol), 1-ethenylpyrrolidin-2-one, poly (hydroxypropyl methacrylate) and their derivatives are also found to be excellent [14, 15, 16, 17, 18, 19, 20, 21]. However, PEOX is relatively less hazardous and viscous in comparison with others, making it a promising substitute for them.

As a part of this research paper, we report the corrosion-inhibitive nature of PEOX, when applied on MS samples along with 0.1 M Hydrochloric acid. To investigate the efficiency of PEOX as corrosion-inhibitor on MS surfaces, experiments based on potentiodynamic polarization (PDP), scanning electron microscopy (SEM), electrochemical impedance spectroscopy (EIS), and measurement of contact angles at the surface are done.

The data based on PDP permits us to determine the kinetics of the total anodic and cathodic processes, when the electrode potential is traced at potentials above and below the open circuit potential, respectively. The PDP technique involves voltage control where the working electrode is polarized at a fixed rate over a given range of potentials. The current flowing through the cell due to the generated electric field is then noted. Using scanning electron microscope (SEM), images of the MS surfaces are produced by scanning the surfaces of MS sample with a focused beam of electrons. These images indirectly convey the extent of protection provided by the PEOX molecules at the surface sites of MS on exposure to corrosion prone environments.

Electrochemical Impedance Spectroscopy (EIS) is generally applied as one of the standard techniques for monitoring corrosion from metallic surfaces. The literature shows that it is used widely for unravelling metallic corrosion and making control strategies for corrosion, particularly corrosion-inhibitors and polymeric coatings.

The measurement of contact angles at the metallic surface assists us to determine the degree of inhibition shown by the PEOX molecules against corrosion at the surface sites of MS. The contact angle (CA) is usually measured through the liquid, where a liquid–vapor interface meets a solid surface, here the surface of MS sample. A given system of solid, liquid, and vapor in nature, at a given temperature and pressure shows a distinctive equilibrium contact angle. If there are changes in the metallic surface sites, it will be reflected in the CA values.

2. Experimental

2.1. Electrolytic solution/medium

The electrolytic solution was prepared from analytical grade HCl (E. Merck, India) using deionized water. All the experiments were done in open air at room temperature and pressure. The inhibitor poly(2-ethyl-2-oxazoline), PEOX (MW ∼ 50,000) was purchased from E. Merck, India. Poly(2-ethyl-2-oxazoline) polymer is amorphous, nonionic, adhesion promoter in coatings and water soluble with good temperature stability. The molecular structure of the inhibitor PEOX is given in Figure 1.

2.2. Materials

The specimens of mild steel (MS) used in this study contains 0.2% C, 1% Mn, 0.03% P, 0.02% S, and 98.75% Fe determined by EDAX method
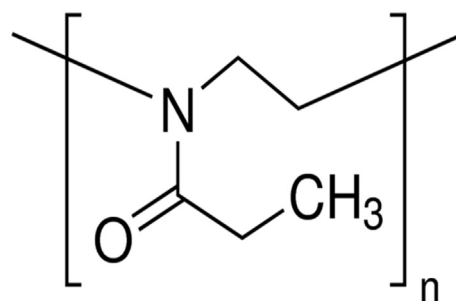

Figure 1. Chemical Structure of poly(2-ethyl-2-oxazoline), PEOX.

(percentage by weight, wt%). To conduct experiments on corrosion, MS specimens with dimensions of 4.8 cm × 1.9 cm × 0.2 cm with $1 cm^2$ area was used as the working electrode. The coupons were rubbed with sand papers having different grit sizes, finally with 2000 grit. Later, the specimens were washed with water, acetone, ethanol, and distilled water in succession and dried in a hot air oven in accordance with instructions of ASTM.

2.3. Electrochemical tests

The analysis of corrosion was performed by CHI 606E Electrochemical Work Station (USA) at 298K. Here, Mild Steel with area 1 cm^2 was taken as the working electrode, Pt foil as the auxiliary electrode and saturated calomel electrode as the reference electrode. The electrochemical data obtained in the experiments were fitted using ZsimpWin software. Before each electrochemical measurement, intense care was given to immerse the working electrode (MS) in 250 ml of 0.1 M HCl solution for an hour to obtain a constant OCP and equilibrium potential. The AC impedance measurements were recorded with an AC amplitude of 10 mV at the corrosion potential in a frequency range of between 0.1 Hz and 10 kHz. The Tafel plots were constructed by perturbing the mild steel working electrode, + 250 mV anodically, and -250 mV cathodically around OCP with a sweep rate of 1 mV/s. Extrapolating the linear portion of the anodic and cathodic Tafel curves to the corrosion potential until they intersect as straight lines to obtain intercept, corrosion current density, cathodic Tafel slope (βc) and anodic Tafel slope (βa) were calculated. Using these values, the efficiency of PEOX as a corrosion-inhibitor was calculated.

2.4. Measurements of contact angles

The measurements of static contact angle for bare MS and MS covered with POX were made by sessile drop method using a contact angle measuring system, Digital Coating Thickness Meter. All experiments were performed at room temperature and pressure. Each analysis was carried out thrice to ensure the accuracy.

2.5. Surface studies

The surface topology of the bare and corroded MS surfaces both in the presence and in the absence of poly(2-ethyl-2-oxazoline) was recorded by SEM with an accelerating voltage of 20.0 kV.

2.6. Theoretical studies

Calculations based on Density Functional Theory (DFT) were done on the monomer, dimer and trimer of PEOX using the model chemistry B3LYP/6-31+G (d, p) for the optimized geometries in aqueous phase. One of the promising quantum chemical computational packages, Gaussian 09 was used for these calculations. The polarizable continuum model (PCM) was applied here to model solvation effects, where the solvent is considered as a polarizable continuum, rather than individual

molecules. Also, frequency analysis, and calculation of molecular orbitals (MOs) and electrostatic potential (ESP) were done for the monomer, dimer and trimer of PEOX in aqueous phase. Some other theoretical parameters which could assist us in the current work were calculated by the following mathematical expressions. Here, the symbols E_{HOMO} and E_{LUMO} denote the energies of the highest occupied molecular orbital and lowest unoccupied molecular orbital respectively.

$$\text{Ionization energy (I) (eV) } I = - E_{HOMO} \tag{1}$$

$$\text{Electron affinity (A) (eV) } A = - E_{LUMO} \tag{2}$$

$$\Delta E = E_{LUMO} - E_{HOMO} \tag{3}$$

$$\text{Back Donation } \left(\Delta E_{bd}\right) = - \frac{(\Delta E)}{8} \tag{4}$$

$$\text{Fraction of Electron Transferred } (\Delta N) = \left(\frac{\chi_{Fe} - \chi_{inhi}}{\eta_{Fe} + \eta_{inhi}}\right) \tag{5}$$

3. Results and discussion

3.1. Studies based on AC impedance spectroscopy

The corrosion-inhibition shown by samples of Mild Steel in the presence of PEOX was studied in 0.1 M Hydrochloric acid solution by AC impedance spectroscopy at 298K, after 1 h of immersion. The AC impedance spectroscopy is also known as dielectric spectroscopy and is based on the analysis of dielectric properties of a medium as function of frequency. The Impedance is a form of resistance that opposes the law of alternating current in a complex system. In this technique, low amplitude alternating current/potential wave is applied. The corrosion process compels the measured current to be out of phase with the input voltage. The Ratio of input potential to the output current will give the value of impedance. The change in the magnitude of impedance/phase angle is used for the interpretation. A great deal of insight is offered by EIS examination on electrochemical interfaces and the results are of great use as the inhibition mechanism is an interfacial process [22]. To obtain sufficient data to explore the mechanism behind the protection shown by PEOX molecules against corrosion, ZsimpWin software was used. From Nyquist plots an equivalent Randles circuit, composed of a solution resistance (R_s), a double layer capacitance (C_{dl}) and charge transfer resistance (R_{ct}) was generated. The most appropriate electrical circuit is presented in Figure 2. Nyquist and Bode plots are the two types of plots which represent the EIS data of electrochemical cells. The Bode plots refer the real and imaginary part of the impedance components/phase angle as a function of frequency. A complex plane/Nyquist plots depicts the imaginary impedance, which is indicative of the capacitive and inductive character of the electrochemical cell versus the real impedance.

The Nyquist plot consists of a depressed semicircle associated with charge transfer resistance of the corrosion process [23, 24, 25, 26]. From Nyquist plots (Figure 3), obtained are not perfect semicircles, which represents the unevenness of mild steel surface, surface inhomogeneities, non-uniformity of the adsorption film and the formation of porous layers [27, 28, 29]. The inhibitor PEOX adsorbs on the MS surface by the replacement of the chemical product (H^+ & Cl^-) and pre-adsorbed water
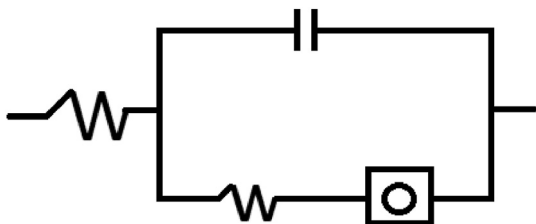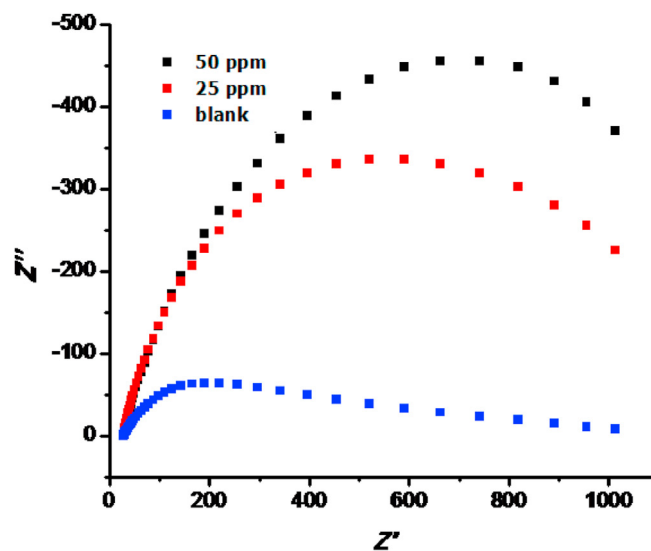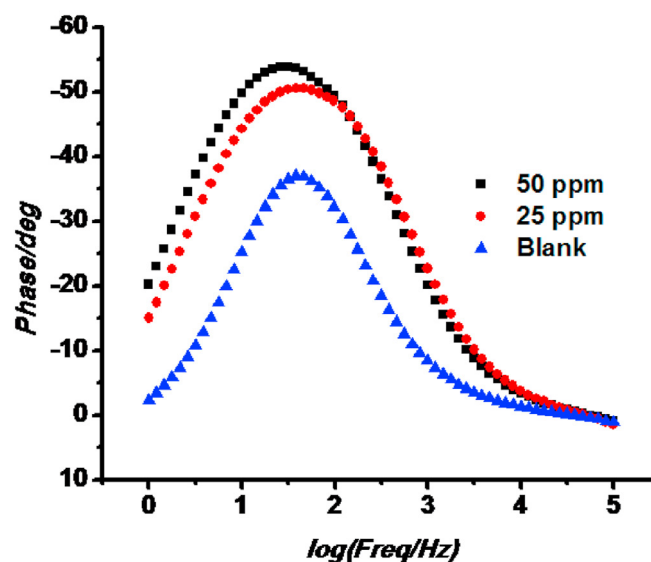

Figure 2. Equivalent circuit compatible with the experimental impedance data.

(a)

(b)

Figure 3. (a) Nyquist plots and (b) Bode phase angle plots of mild steel in 0.1 N HCl with various concentrations PEOX.

molecules [30]. The adsorption of the inhibitor increases with increase in its concentration and the corresponding rise in resistance at the interface between metal and electrolyte. The stepwise increase in the resistance develops a better barrier protection against the mass and charge transfer processes at the metal electrolyte interfaces.

The C_{dl} values decrease with increase in the concentration of PEOX while the R_{ct} values increase with inhibitor concentration (Table 1). The decrease of C_{dl} values is related to the decline in local dielectric constant or increase in the thickness of the protective layer. An increment in the diameters of capacitive loop in the Nyquist plots indicates the formation of inhibitive layer on the surface of Mild Steel. The shape and nature of Nyquist plots remains same even after the addition of the inhibitor. The chi-square values between the fitted values and measured values are small and are less than of the order of 0.01. When the inhibitor, PEOX molecules were added to 0.1 M HCl solution, the phase angle was changed to more negative values, followed by the enhancement of capacitive behavior indicating the adsorption of the inhibitor. Also, it was observed that the phase angles were moved to more negative values

Table 1. Electrochemical parameters in 0.1 N HCl for mild steel with and without POX.

Conc:	R_s (Ωcm^{-2})	R_{ct} (Ωcm^{-2})	R_i (Ωcm^{-2})	C_{dl} ($\mu F\ cm^{-2}$)	CPE ($\mu\ \Omega^{-1}\ cm^{-2}\ s^n$)	IE %
Blank	29.55	160.2	14.34	26.98	10.34×10^{-5}	–
25 ppm	27.7	1035	30.22	9.307	10.10×10^{-5}	84.52
50 ppm	28.24	1353	4.58	2.878	9.74×10^{-5}	88.15

as a function of the inhibitor concentration [26, 27, 28, 29, 30]. The double layer capacitance (C_{dl}) value reduces from 26.98 to 2.878 µF cm^{-2} as the concentration of the inhibitor increased to 50 ppm which indicates that the charge and discharge rates of ions to the metal–solution interface is greatly diminished.

3.2. Potentiodynamic polarization measurements (PDP)

The PDP analyses are chiefly used to check the efficiency of inhibitor in corrosive medium [31, 32]. The PDP is depicted in the form of Tafel curve and Tafel plot for bare mild steel, with different concentration of PEOX in 0.1 M HCl medium (Figure 4).

The PDP measurements provided anodic and cathodic polarization curves for the corrosion process of MS in 0.1M HCl. For determining the corrosion current densities (I_{corr}), the slopes of the Tafel curves were extrapolated to corrosion potential. From Table 2, it can be observed that the addition of PEOX shows a positive movement in the E_{corr} value. According to Li et al [33], the inhibitor performs as either anodic or cathodic type when the change in corrosion potential exceeds ±85 mV with respect to corrosion potential of the uninhibited solution. In the present study, the shift in E_{corr} value is found to be < ±85 mV. The values of bare MS and MS with PEOX increased from –514 mV versus reference electrode and −490, −476 mV versus reference electrode. It implies that PEOX molecules perform as a mixed-type inhibitor and their inhibitory action on both hydrogen evolution and metal dissolution [33, 34]. The enhanced resistance of PEOX towards corrosion is confirmed by shift towards the +ve region. This is further proved by the reduction in corrosion current density (I_{corr}) values from 448.8 µAcm^{-2} to 90.8 µAcm^{-2}. Thus, addition of this inhibitor not only reduces the iron dissolution but also impede the hydrogen evolution process. In the anodic region of Tafel curve PEOX is found to be attached on the MS surface, thus arresting the available reaction sites. The surface coverage increases with the PEOX concentration. The corrosion parameters derived from these curves are listed in Table 2. The formation of a barrier film on the MS surface can be concluded from the decrease in the
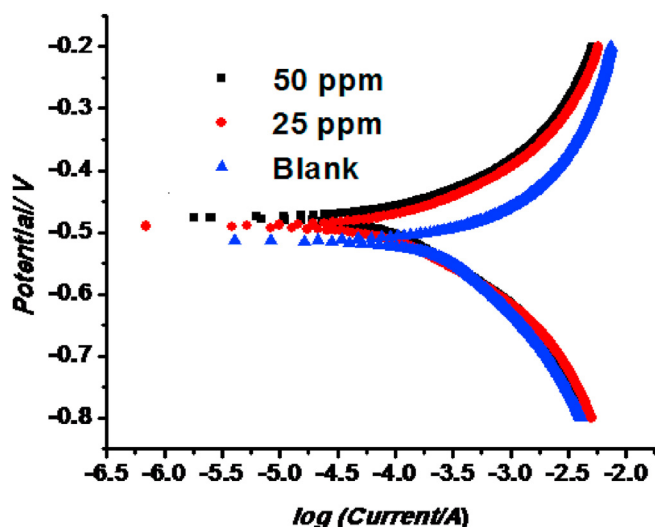
corrosion rate (CR) and corrosion current density (I_{corr}) values with increasing concentration of the inhibitor. The percentage protection efficiency (IE%) is calculated according to the following equation [35].

$$\%IE = \frac{I_{corr^*} - I_{corr}}{I_{corr^*}} \times 100 \qquad (6)$$

where, I_{corr^*} and I_{corr} are the corrosion current densities of bare MS with and without the addition of inhibitor EPOX.

3.3. Measurements on contact angles

By measuring the static contact angle one can confirm and verify the deposition of PEOX film on MS surface and it is influenced by the polar nature of the liquid, the polarity of the surface sites, contamination at the metallic surface, and roughness of the surface. Figure 5 indicates the morphological appearance of mild steel surfaces before and after immersion in 0.1 M HCl solutions with different concentrations of PEOX at room temperature.

The contact angle of water droplets was 68.3° which indicated the hydrophilic nature of bare MS surface. The contact angle of water droplets was dropped from 68.3° to 50.6° when exposed to 0.1 M HCl showing that the surface was harshly damaged considerably in the corrosive medium. The presence of the polymer PEOX was found to impart hydrophobic nature to the metallic surface. The contact angle of water droplets was increased from 50.6° to 65.1° and 71.4° as indicated in figures 4c & d. The results suggest that the inhibitor competently shields the MS surface and thus leads to prevent the metal from corrosive attack [36, 37].

3.4. Morphological studies

To understand the efficiency of PEOX on MS surface as a corrosion-inhibitor, morphological examinations were carried out using SEM. Figures 6a & 6b depict SEM images of bare MS before and after immersion in acid without inhibitor PEOX for 96 h. This micrograph shows the effect of acid on MS specimens. Figure 6c shows the SEM image of the surface of mild steel dipped in the electrolyte containing 50 ppm of PEOX which reveals that the surface is free from cracks, and appears to be free from roughness. It can be concluded that corrosion is very low in the presence of the inhibitor and the appearance of smooth surface obtained in the presence of PEOX proves its higher efficiency of corrosion-inhibition. The development of a layer of protective barrier on the surface of MS inhibits the penetration of attacking species from the corrosive medium, and the corrosion is negligible.

3.5. Quantum chemical calculations

The effect of electronic structure on the prevention of corrosion shown by PEOX is traced by DFT calculations done on the monomer, dimer and trimer in the gaseous form and in aqueous phase. The optimized geometries in each case are obtained, and some of the quantum chemical parameters which are useful in interpreting the role of PEOX as a corrosion-inhibitor are calculated. It includes the identification of highest occupied molecular orbital (HOMO), lowest unoccupied molecular orbital (LUMO) and the maps of electrostatic potential as contours (ESP) for monomer, dimer and trimer. These are calculated using the model chemistry, B3LYP/6-31+G (d, p) and are presented in Figure 7.

Figure 4. PPD plots for MS corrosion in 0.1 M HCl containing various concentrations of PEOX.

Table 2. PDP parameter in 0.1 N HCl for mild steel with and without POX.

Conc	$-E_{corr}$ (mV)	LPR(Ω)	β_a (mV/dec)	$-\beta_c$ (mV/dec)	I_{corr} (μAcm^{-2})	IE %
Blank	514	82	6.067	5.815	448.8	–
25 ppm	490	219	8.810	8.938	112.0	75.04
50 ppm	476	229	8.309	8.826	90.8	79.76

(a)

(c) 25 ppm

(b)
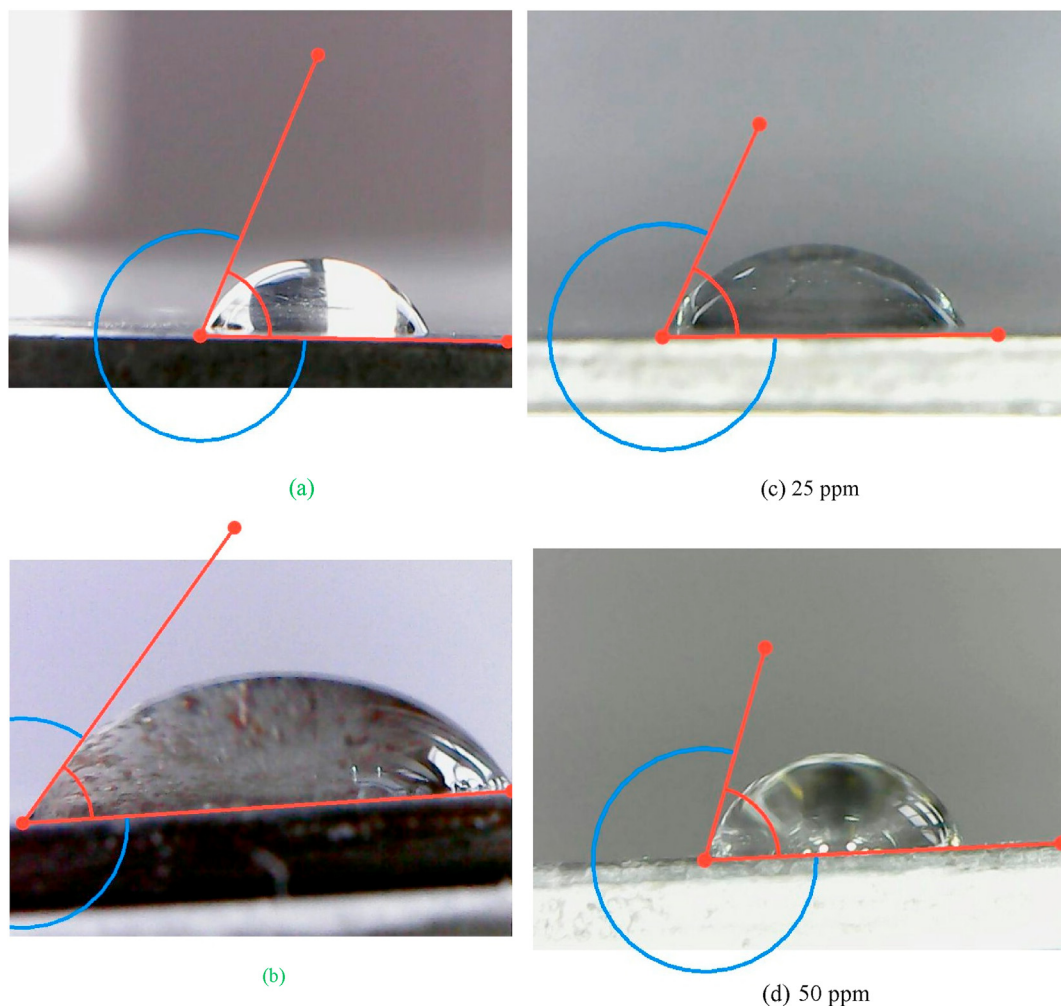
(d) 50 ppm

Figure 5. Contact angle measurements of water droplets on (a) Bare MS; (b) after 24 h immersion of MS in 0.1 M HCl; (c) after 24 h immersion of MS in 0.1 M HCl with 25 ppm PEOX and (d) after 24 h immersion of MS in 0.1 M HCl with 50 ppm of PEOX.

The values of dipole moment (μ) and the energy gap (ΔE) between HOMO and LUMO of PEOX molecules indirectly convey the extent of their interaction with the metallic surface and are listed in Table 3. Literature shows that E_{HOMO} of the inhibitor molecule is a direct indication of the tendency to donate electrons to acceptor atoms, and E_{LUMO} is measure of accepting electrons into its LUMO from a suitable donor molecule. The difference in these values, $E_{LUMO} - E_{HOMO}$, represents the chemical reactivity of the inhibitor molecule, and a relatively low value of ΔE indicates eagerness for chemical reactivity and hence a better efficiency for corrosion-inhibition [38]. The following expression provides a method to estimate the fraction of electrons transferred (ΔN) from a molecule of the inhibitor to the metallic surface.

$$\Delta N = \left(\frac{\chi_{Fe} - \chi_{inhi}}{\eta_{Fe} + \eta_{inhi}} \right)$$

Here χ_{Fe} and χ_{inhi} represent the total electronegativity of iron atom and the inhibitor molecule, respectively; η_{Fe} and η_{inhi} represents the

absolute hardness of iron atom and the inhibitor molecule. These quantities are directly correlated to electron affinity (A) and ionization potential (I) of the corresponding molecular systems as shown below.

$$\chi = \frac{I + A}{2} \tag{7}$$

and

$$\eta = \frac{I - A}{2} \tag{8}$$

Using Koopman's theorem, the I and A are related to the frontier orbital energies as, $I = E_{HOMO}$ and $A = -E_{LUMO}$. Also, the absolute electronegativity of iron atom, χ_{Fe} is 7 eV mol^{-1} and the absolute hardness of iron η_{Fe} is 0 eV mol^{-1}. It is reported that a value of ΔN which is less than 3.6 shows the increased inhibition efficiency of the inhibitor arising from electron-donating ability of the inhibitor to the iron surface
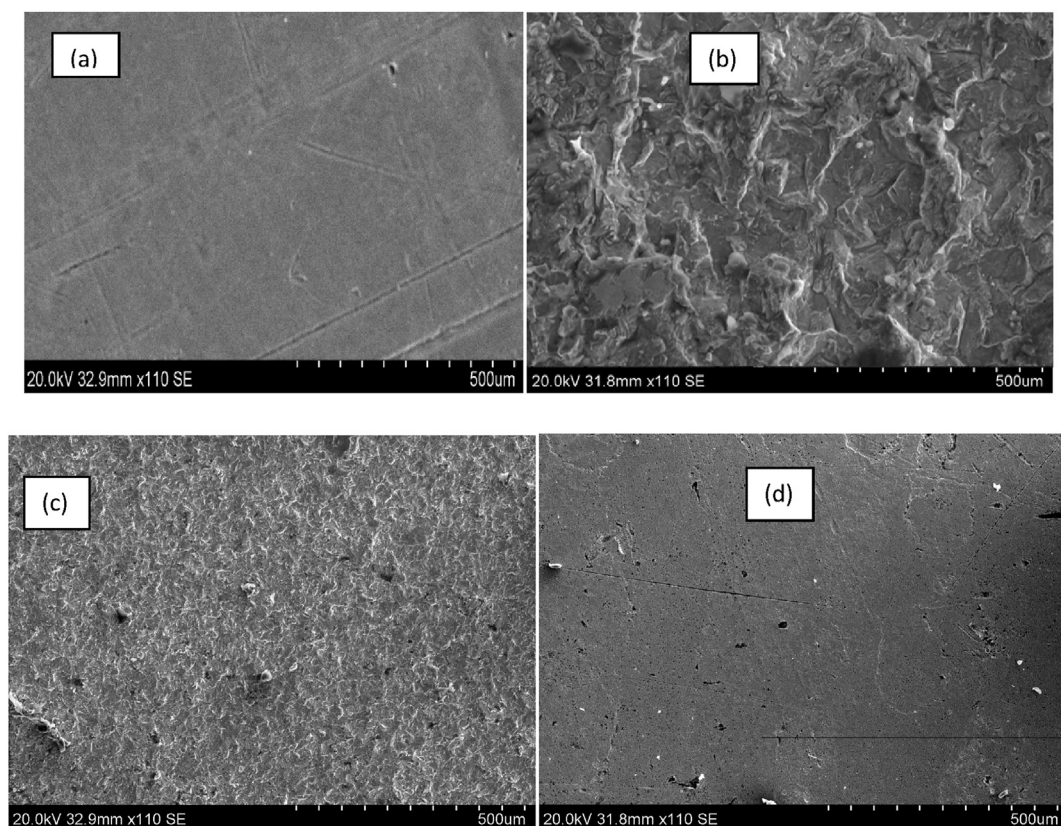
Figure 6. SEM images of (a) bare MS, (b) in 0.1M HCl without inhibitor; (c) in the presence of 25 ppm of PEOX and (d) in the presence of 50 ppm of PEOX after 24 Hour.
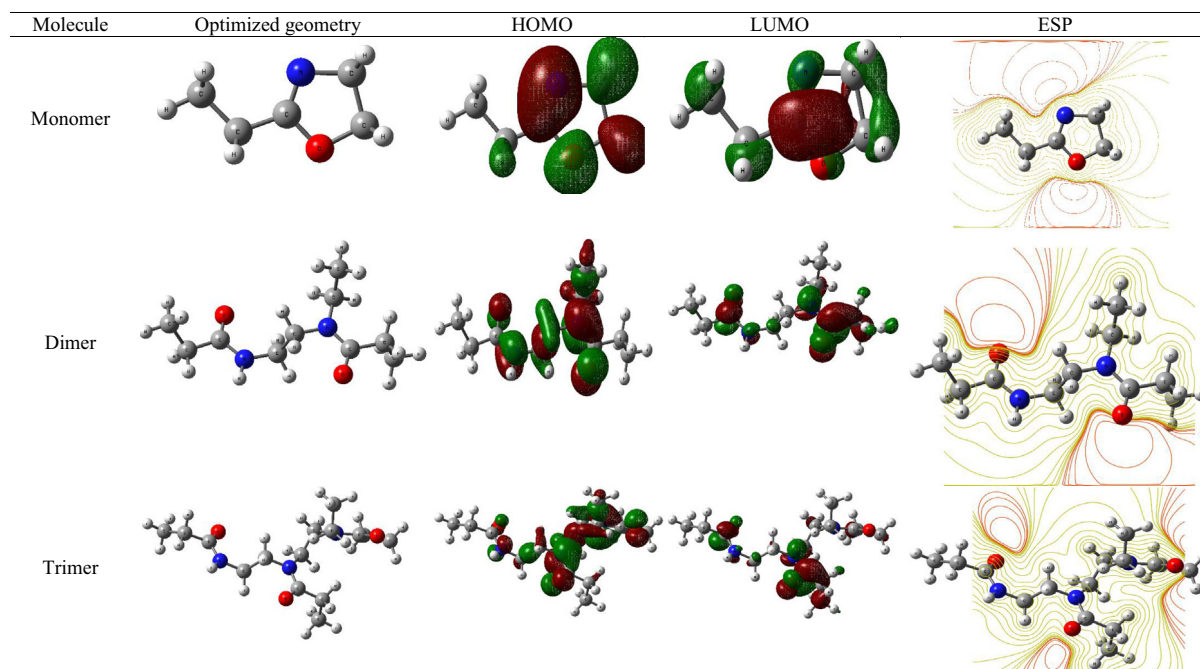
Figure 7. The optimized geometries, frontier molecular orbitals, and electrostatic potential maps for monomer, dimer and trimer of PEOX.

Table 3. Calculated theoretical parameters of presented POX in aqueous media.

Parameter	Monomer	Dimer	Trimer
E_{HOMO} (eV)	-5.4260	-5.2555	-5.1367
E_{LUMO} (eV)	-0.1204	-0.0942	-0.2022
ΔE (eV)	5.3056	5.1613	4.9345
I (eV)	5.4260	5.2555	5.1367
A (eV)	0.1204	0.0942	0.2022
χ_{inhi} (eV)	2.7725	2.6748	2.6764
η_{inhi} (eV)	2.6520	2.5806	2.4662
χ_{Fe} (eV)	7	7	7
η_{Fe} (eV)	0	0	0
ΔE_{b-d} (eV)$^{-1}$	-0.6632	-0.6569	-0.6168
μ(D)	1.799	0.848	4.673
ΔN	0.7970	0.8380	0.8765
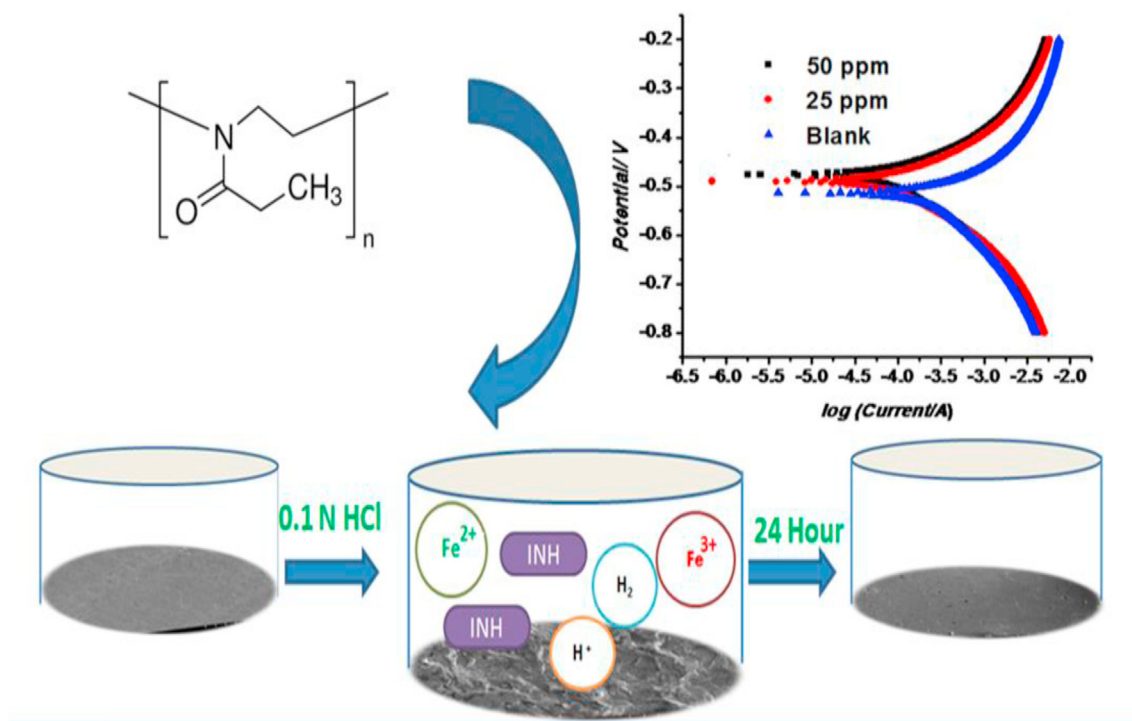
Figure 8. The proposed Schematic representation of inhibition by PEOX.

[38]. The calculated ΔN values for the monomer, dimer and trimer are 0.79, 0.83 and 0.89 respectively, which confirm the experimental explanations. The schematic representation of inhibition by PEOX is shown in Figure 8.

4. Conclusions

- In the present investigation a new, eco-friendly and cost-effective polymer, PEOX, is used as a corrosion-inhibitor.
- The molecules of PEOX are found to be effective in hindering the dissolution of MS in 0.1 M HCl solution.
- The AC impedance analysis, PDP studies and contact angle measurements show efficient protection against corrosion.
- The addition of the polymer PEOX changes the double layer capacitance at the metal-solution interface and it is due to the adsorption of the inhibitor molecules on MS surface.

- Suppressing both anodic and cathodic reactions, the polymer PEOX can be considered as a mixed type inhibitor, as it influences both anodic and cathodic branches of Tafel curves.
- The EIS measurements proves that increasing the concentration of the PEOX increases inhibition against corrosion at the surfaces of MS samples in 0.1 M HCl solution.

Declarations

Author contribution statement

Sam John: Contributed reagents, materials, analysis tools or data; Wrote the paper.

Data availability statement

The authors do not have permission to share data.

Declaration of interests statement

The authors declare no conflict of interest.

Additional information

No additional information is available for this paper.

References

[1] H. Jensen, G. Sorensen, Ion bombardment of nano-particle coatings, Surf. Coating. Technol. 84 (1996) 500–505.

[2] P. Droniou, W.E. Fristad, Li.J. Liang, Nanoceramic based conversion coating in the paint shop, Coatings 38 (2005) 237–239.

[3] G.X. Shen, Y.C. Chen, L. Lin, C.J. Lin, D. Scantlebury, Study on a hydrophobic nano-TiO₂ coating and its properties for corrosion protection of metals, Electrochim. Acta. 50 (2005) 5083–5089.

[4] F. Euler, C. Jakob, H. Romanus, L. Spiess, B. Wielage, T. Lampke, S. Steinha, Interface behavior in nickel composite coatings with nano-particles of oxide ceramic, Electrochim. Acta. 48 (2003) 3063–3070.

[5] T.K. Rout, G. Jha, A.K. Singh, N. Bandyopadhyay, O.N. Mohanty, Development of conducting polyaniline coating: a novel approach to superior corrosion resistance, Surf. Coating. Technol. 167 (2003) 16–24.

[6] B. Wessling, J. Posdorfer, Nanostructures of the dispersed organic metal polyaniline responsible for macroscopic effects in corrosion protection, Synth Met 102 (1999) 1400–1401.

[7] B. Garcia, A. Lamzoudi, F. Pillier, H.N.T. Le, C. Deslouis, Oxide/polypyrrole composite films for corrosion protection of iron, J.Electrochem. Soc. 149 (2002) 52–60.

[8] J.M. Yeh, C.P. Chin, Structure and properties of poly (o-methoxyaniline)-clay nano-composite materials, J. Appl. Polym. Sci. 88 (2003) 1072–1078.

[9] M. Lebrini, M. Lagrene, H. Vezin, L. Gengembre, F. Bentiss, Electrochemical and quantum chemical studies of new thiadiazole derivatives adsorption on mild steel in normal hydrochloric acid medium, Corros. Sci. 47 (2005) 485–505.

[10] X. Wang, H. Yang, F. Wang, An investigation of benzimidazole derivative as corrosion inhibitor for mild steel in different concentration HCl solutions, Corros. Sci. 53 (2011) 113–121.

[11] F.B. Growcock, Inhibition of Steel Corrosion in HCl by derivatives of Cinnamaldehyde Part I. Corrosion inhibition model, Corrosion 45 (1989) 1003–1007.

[12] A. Pourghasemi Hanza, R. Naderi, E. Kowsari, M. Sayebani, Corrosion behavior of mild steel in H₂SO₄ solution with 1,4-di [1′-methylene-3′-methyl imidazolium bromide]-benzene as an ionic liquid, Corros. Sci. 107 (2016) 96–106.

[13] A.A. Fathima Sabirneeza, R. Geethanjali, S. Subhashini, Polymeric corrosion inhibitors for iron and its alloys: A review, Chem. Eng. Commun. 202 (2015) 232–244.

[14] B. Muller, G. Kubitzki, G. Kinet, Aromatic 2-hydroxy-oximes as corrosion inhibitors for aluminium and zinc pigments, Corros. Sci. 40 (1998) 1469–1477.

[15] E. Ghali, Corrosion Resistance of Aluminum and Magnesium Alloys, A John Wiley& sons INC, publication, United States of America, 2010, https://doi.org/10.1002/9780470531778.

[16] E.E. Ebenso, U.J. Ekpe, S.A. Umoren, E. Jackson, O.K. Abiola, N.C. Oforka, Synergistic effect of halide ions on the corrosion inhibition of aluminum in acidic medium by some polymers, J. Appl. Polym. Sci . 100 (2006) 2889–2894.

[17] S.A. Umoren, Synergistic inhibition effect of polyethylene glycol-polyvinyl pyrrolidone blends for mild steel corrosion in sulphuric acid medium, J. Appl. Polym. Sci . 119 (2011) 2072–2084.

[18] L. Garrigues, N. Pebere, F. Dabosi, An investigation of the corrosion inhibition of pure aluminum in neutral and acidic chloride solutions, Electrochim. Acta. 41 (1996) 1209–1215.

[19] S.A. Umoren, E.E. Ebenso, P.C. Okafor, U.J. Ekpe, O. Ogbobe, Effect of halide ions on the corrosion inhibition of aluminium in alkaline medium using polyvinyl alcohol, J. Appl. Polym. Sci. 103 (2007) 2810–2816.

[20] S.A. Umoren, U.M. Eduok, Application of carbohydrate polymers as corrosion inhibitors for metal substrates in different media: A review, Carbohydr. Polym. 140 (2016) 314–341.

[21] U. Riaz, S.M. Ashraf, S. Ahmad, High performance corrosion protective DGEBA/polypyrrole composite coatings, Prog. Org. Coatings 59 (2007) 138–145.

[22] A.F.S. Abdul Rahiman, S. Sethumanickam, Corrosion inhibition, adsorption and thermodynamic properties of poly(vinyl alcohol-cysteine) in molar HCl, Arab. J. Chem. 10 (2017) S3358–S3366.

[23] K.S. Jacob, G. Parameswaran, Corrosion inhibition of mild steel in hydrochloric acid solution by Schiff base furoin thiosemicarbazone, Corros. Sci. 52 (2010) 224–228.

[24] S. Deng, X. Li, H. Fu, Nitrotetrazolium blue chloride as a novel corrosion inhibitor of steel in sulfuric acid solution, Corros. Sci. 52 (2010) 3840–3846.

[25] S. John, A. Joseph, A. James, B. Narayana, Enhancement of corrosion protection of mild steel by chitosan / ZnO nanoparticle composite membranes, Prog. Org. Coatings 84 (2015) 28–34.

[26] P. Bommersbach, C. Alemany-Dumont, J.P. Millet, B. Normand, Hydrodynamic effect on the behaviour of a corrosion inhibitor film: Characterization by electrochemical impedance spectroscopy, Electrochim. Acta. 51 (2006) 4011–4018.

[27] M. Sikine, Y.K. Rodi, H. Elmsellem, O. Krim, H. Steli, Y. Ouzidan, A.K. Rodi, F.O. Chahdi, N.K. Sebbar, E.M. Essassi, Inhibition Study of Mild Steel Corrosion in Hydrochloric Acid by 1 , 5- Benzodiazepine-2 , 4-dione, J. Mater. Environ. Sci. 7 (2016) 1386–1395.

[28] K.F. Khaled, Experimental, density function theory calculations and molecular dynamics simulations to investigate the adsorption of some thiourea derivatives on iron surface in nitric acid solutions, Appl. Surf. Sci. 256 (2010) 6753–6763.

[29] A. Zouitini, Y.K. Rodi, H. Elmsellem, H. Steli, F.O. Chahdi, M.A. Shariati, A.E. Janati, Y. Ouzidan, N.K. Sebbar, E.M. Essassi, Experimental and theoretical studies on inhibition of Quinoxaline derivatives against corrosion of mild steel in acidic medium, J Mater. Environ. Sci. 8 (2017) 4105–4116.

[30] D. Borisova, D. Akçakayiran, M. Schenderlein, H. Möhwald, D.G. Shchukin, Nanocontainer-based anticorrosive coatings: Effect of the container size on the self-healing Performance, Adv. Funct. Mater. 23 (2013) 3799–3812.

[31] M. Lagrenée, B. Mernari, M. Bouanis, M. Traisnel, F. Bentiss, Study of the mechanism and inhibiting efficiency of 3,5-bis(4-methylthiophenyl)-4H-1,2,4-triazole on mild steel corrosion in acidic media, Corros. Sci. 44 (2002) 573–588.

[32] H. Habazaki, T. Kimura, Y. Aoki, E. Tsuji, T. Yano, Highly Enhanced Corrosion Resistance of Stainless Steel by Sol-Gel Layer-by-Layer Aluminosilicate Thin Coatings, J. Electrochem. Soc. 161 (2013) C57–C61.

[33] W. Li, Q. He, C. Pei, B. Hou, Characterization of ceramic sol-gel coatings as an alternative chemical conversion treatment on commercial carbon steel, Electrochim. Acta. 52 (2007) 6386–6394.

[34] M.A. Dominguez-Crespo, A. Garcia-Murillo, A.M. Torres-Huerta, F.J. Carrillo-Romo, E. Onofre-Bustamante, C. Yanez-Zamora, Experimental and theoretical investigation of the adsorption behavior of new triazole derivatives as inhibitors for mild steel corrosion in acid media, Electrochim. Acta 54 (2009) 2932–2940.

[35] W.H. Li, Q. He, S.T. Zhang, C.L. Pei, B.R. Hou, Some new triazole derivatives as inhibitors for mild steel corrosion in acidic medium, J. Appl. Electrochem. 38 (2008) 289–295.

[36] A.S. Fouda, Role of Some Organic Compounds as Corrosion Inhibitors for 316L Stainless Steel in 1 M HCl, Int. J. Electrochem. Sci. 12 (2017) 347–362.

[37] M. Abdallah, M.M. Salem, B.A. AL Jahdaly, M.I. Awad, E. Helal, A.S. Fouda, Corrosion inhibition of stainless-steel type 316 L in 1.0 M HCl solution using 1,3-thiazolidin-5-one derivatives, Int. J. Electrochem. Sci. 12 (2017) 4543–4562.

[38] S.K. Saha, A. Dutta, P. Ghosh, D. Sukul, P. Banerjee, Novel Schiff-base molecules as efficient corrosion inhibitors for mild steel surface in 1 M HCl medium: experimental and theoretical approach, Phys. Chem. Chem. Phys. 18 (2016) 17898–17911.